OPTIMIZED ROBOTIC MEDICINE-DISPENSING ARM

A PROJECT REPORT

Submitted by

NEELAMBARI P	DL.AI.U4AID24026
ARUNIMA KRISHNA	DL.AI.U4AID24008
ARPIT BARAL	DL.AI.U4AID24007

In partial fulfilment for the award of the degree of

BACHELOR OF TECHNOLOGY (B. Tech)

in

ARTIFICIAL INTELLIGENCE AND DATA SCIENCE (ME)

Under the guidance of

Dr.Anirban Tarafdar

Prof.Jayaprakash

Submitted to

AMRITA VISHWA VIDYAPEETHAM
AMRITA SCHOOL OF ARTIFICIAL INTELLIGENCE

FARIDABAD – 121002

December 2025

BONAFIDE CERTIFICATE

This is to certify that this project report entitled **" Optimized Robotic Medicine-Dispensing Arm "** is the bonafide work of Neelambari P (DL.AI.U4AID24026), Arunima Krishna (DL.AI.U4AID24008), Arpit Baral (DL.AI.U4AID24007) who carried out the project work under my supervision.

SIGNATURE

Dr.Anirban Tarafdar
Prof.Jayaprash
School of AI
Faridabad

DECLARATION BY THE CANDIDATE

I declare that the report entitled **" Optimized Robotic Medicine-Dispensing Arm "** submitted by me for the degree of Bachelor of Technology is the record of the project work carried out by me under the guidance of Dr.Anirban Tarafdar and Prof.Jayaprakash and this work has not formed the basis for the award of any degree, diploma, associateship, fellowship, title in this or any other University or other similar institution of higher learning.

SIGNATURE

NEELAMBARI P	DL.AI.U4AID24026
ARUNIMA KRISHNA	DL.AI.U4AID24008
ARPIT BARAL	DL.AI.U4AID24007

ACKNOWLEDGEMENT

This project work would not have been possible without the contribution of many people. It gives me immense pleasure to express my profound gratitude to our honorable Chancellor Sri Mata Amritanandamayi Devi for her blessings and inspiration. I extend my sincere gratitude to our Principal, Dr. Lakshmi Mohandas, Amrita School of Artificial Intelligence, for providing facilities and academic support.

I express my sincere thanks to my supervisor Dr.Anirban Tarafdar and Prof.Jayaprakash for his constant guidance, encouragement, and technical insight throughout the course of this work.

NEELAMBARI P	DL.AI.U4AID24026
ARUNIMA KRISHNA	DL.AI.U4AID24008
ARPIT BARAL	DL.AI.U4AID24007

TABLE OF CONTENTS

1 Introduction 5
2 Objectives 6
3 Methodology / Work Done 7
3.1 Mechanical Configuration: SCARA Manipulator 7
3.2 Forward Kinematics Modeling 8
3.3 Inverse Kinematics via Optimization 8
3.3.1 Cost Function Formulation 8
3.3.2 Jacobian Matrix Derivation 8
3.3.3 Iterative Update Rule 9
3.4 Dynamic Modeling Using Euler–Lagrange Formulation 9
3.4.1 Gravity Compensation 9
3.4.2 Rotational Dynamics 10
3.5 Trajectory Generation 10
4 Results and Discussion 11
4.1 Simulation Scenario and Parameters 11
4.2 Kinematic Performance Analysis 11
4.2.1 Optimization Convergence 11
4.2.2 Three-Dimensional Path Visualization 11
4.3 Dynamic Performance Analysis 12
4.3.1 Gravity Compensation and Payload Detection 12
4.3.2 Torque Smoothness 13
4.4 Velocity and Momentum Analysis 13
4.4.1 S-Curve Velocity Profiles 13
4.4.2 Angular Momentum Behavior 13
4.5 Summary of Findings 14
5 Future Scope 15
5.1 Computer Vision Integration 15
5.2 Reinforcement Learning for Advanced Path Planning 15
5.3 Mathematical Obstacle Avoidance 15
5.4 IoT Connectivity and Swarm Coordination 16
6 Conclusion 17
References 18

1 Introduction

The healthcare sector is increasingly adopting automation to address critical operational inefficiencies, particularly within hospital pharmacies where manual medication dispensing remains highly error-prone. Studies indicate that human involvement in medication handling is associated with an error rate ranging from 1.5% to 5%, often resulting in dosage inaccuracies and contamination of sterile pharmaceutical compounds [2]. Given the safety-critical nature of healthcare environments, even minor dispensing errors can lead to serious risks to patient safety, highlighting the need for reliable and precise automated solutions.

Although robotic automation has improved dispensing accuracy, most conventional robotic systems rely on rigid, pre-programmed geometric trajectories. Such approaches lack adaptability in dynamic and cluttered hospital environments, where workspace constraints, variable payloads, and frequent task reconfiguration are common [2]. As a result, these systems often struggle to maintain smooth motion and numerical stability under real-world operating conditions, particularly near kinematic singularities and workspace boundaries.

To overcome these limitations, this project presents an Optimized Robotic Medicine-Dispensing Arm that replaces manual intervention with a high-precision automated workflow. The proposed system employs a 4-degree-of-freedom (DOF) SCARA manipulator and formulates the inverse kinematics problem as a Jacobian-based gradient descent optimization task rather than relying on analytical trigonometric solutions [12, 13]. By iteratively minimizing the Euclidean distance between desired and actual end-effector positions, the system achieves sub-millimeter accuracy while avoiding kinematic singularities [28]. Furthermore, a physics-aware dynamic model based on the Euler–Lagrange formulation ($L = T - V$) enables real-time torque computation and gravity compensation, ensuring mechanically stable and jerk-free motion even when handling variable payloads such as a 0.2 kg medicine bottle.

2 Objectives

The primary objective of this project is to design, simulate, and evaluate a robust control framework for a robotic manipulator intended for pharmaceutical dispensing applications. Unlike conventional geometry-based controllers, the proposed system emphasizes mathematical optimization and physics-aware dynamic modeling to achieve precise, stable, and safe robotic operation in healthcare environments.

The specific technical objectives of this work are outlined below:

- **Optimization-Based Inverse Kinematics:** To formulate the inverse kinematics (IK) problem as a numerical optimization task using a Jacobian-based gradient descent algorithm. By minimizing a defined cost function representing end-effector position error, the system aims to achieve improved adaptability and avoid kinematic singularities associated with closed-form solutions.

- **Dynamic Modeling Using Euler–Lagrange Formulation:** To develop a physics-aware control model based on the Euler–Lagrange equation ($L = T - V$), incorporating real-time computation of kinetic and potential energy. This objective includes accurate torque estimation and gravity compensation to ensure mechanical stability along the Z-axis.

- **Payload-Aware Control for Medical Safety:** To analyze the dynamic effects of handling variable payloads by simulating the addition of a 0.2 kg medicine bottle at the end-effector. The goal is to ensure that the control system dynamically adjusts joint forces to maintain stability without oscillation, sagging, or loss of precision.

- **Smooth and Jerk-Free Trajectory Generation:** To implement quintic polynomial interpolation for trajectory planning, ensuring continuous velocity and acceleration profiles. This approach aims to eliminate abrupt motion transitions, thereby preventing spillage or damage to fragile pharmaceutical containers during high-speed operations.

- **Three-Dimensional Visualization and Motion Verification:** To develop a comprehensive MATLAB-based simulation environment that visualizes the 4-DOF manipulator in 3D space. This includes tracking the end-effector trajectory and verifying precise gripper orientation control (Joint 4) for accurate object placement.

3 Methodology / Work Done

This chapter presents the complete mathematical and computational framework developed for controlling the proposed robotic medicine-dispensing manipulator. The system architecture is organized into three tightly integrated modules: mechanical configuration, kinematic optimization, and physics-based dynamic modeling. This modular design ensures both computational robustness and physical realism during operation.

3.1 Mechanical Configuration: SCARA Manipulator

The robotic architecture adopted in this project is the **Selective Compliance Assembly Robot Arm (SCARA)**, widely used in high-speed pick-and-place applications due to its planar flexibility and vertical rigidity [3, 6]. This configuration is particularly suitable for pharmaceutical environments where precision, repeatability, and smooth vertical motion are critical.

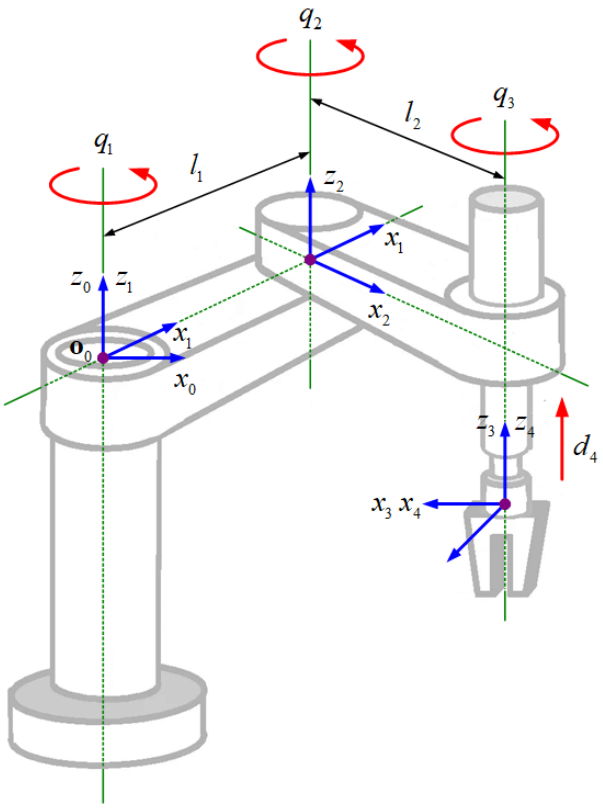

Figure 1: SCARA robot manipulator

The modeled system consists of four degrees of freedom (DOF), defined as follows:

- **Joint 1 (Revolute – Shoulder):** Provides rotation about the Z-axis and enables primary horizontal positioning.

- **Joint 2 (Revolute – Elbow):** Extends the reachable workspace by rotating relative to Link 1.
- **Joint 3 (Prismatic – Vertical):** A linear joint (d_3) responsible for vertical dispensing motion [4].
- **Joint 4 (Revolute – Wrist):** Controls end-effector orientation (θ_4), enabling correct payload alignment [5].

3.2 Forward Kinematics Modeling

To establish deterministic control over the manipulator, a forward kinematics (FK) model was derived using Denavit–Hartenberg (DH) conventions. The FK equations map joint space variables to Cartesian end-effector coordinates (x, y, z) as follows:

$$x = a_1 \cos(\theta_1) + a_2 \cos(\theta_1 + \theta_2) \tag{1}$$

$$y = a_1 \sin(\theta_1) + a_2 \sin(\theta_1 + \theta_2) \tag{2}$$

$$z = d_0 - d_3 \tag{3}$$

Here, a_1 and a_2 denote the shoulder and elbow link lengths (0.35 m and 0.30 m respectively), while d_0 represents the base offset (0.18 m) [7–9].

3.3 Inverse Kinematics via Optimization

Unlike conventional closed-form geometric approaches, inverse kinematics (IK) in this project is formulated as a constrained numerical optimization problem. This design choice enhances numerical stability and avoids singular configurations commonly encountered in analytical solutions.

3.3.1 Cost Function Formulation

A scalar cost function $E(q)$ is defined as the squared Euclidean distance between the current end-effector position and the desired target position:

$$E(q) = \|P_{\text{target}} - P_{\text{current}}(q)\|^2 \tag{4}$$

The objective of the IK solver is to iteratively minimize $E(q)$ until convergence.

3.3.2 Jacobian Matrix Derivation

To guide the optimization process, the Jacobian matrix J is derived, representing the sensitivity of end-effector position with respect to joint variables [10, 11]:

$$J = \begin{bmatrix} \frac{\partial x}{\partial \theta_1} & \frac{\partial x}{\partial \theta_2} & 0 \\ \frac{\partial y}{\partial \theta_1} & \frac{\partial y}{\partial \theta_2} & 0 \\ 0 & 0 & -1 \end{bmatrix} \tag{5}$$

In the MATLAB implementation, the Jacobian is evaluated dynamically as:

$$J = \begin{bmatrix} -a_1 s_1 - a_2 s_{12} & -a_2 s_{12} & 0 \\ a_1 c_1 + a_2 c_{12} & a_2 c_{12} & 0 \\ 0 & 0 & -1 \end{bmatrix} \tag{6}$$

where $s_{12} = \sin(\theta_1 + \theta_2)$ and $c_{12} = \cos(\theta_1 + \theta_2)$.

3.3.3 Iterative Update Rule

Joint variables are updated using the Jacobian transpose gradient descent method [14]:

$$q_{\text{new}} = q_{\text{old}} + \alpha J^T \left(P_{\text{target}} - P_{\text{current}} \right) \tag{7}$$

The learning rate α is set to 0.05, and iterations continue until the position error norm falls below 10^{-5} m [15].

3.4 Dynamic Modeling Using Euler–Lagrange Formulation

To ensure physically realistic motion, the system integrates dynamic modeling based on the Euler–Lagrange formulation:

$$L = T - V \tag{8}$$

This module computes required motor torques in real time while operating alongside the kinematic solver [16].

3.4.1 Gravity Compensation

The prismatic joint (Joint 3) operates along the vertical axis and must counter gravitational forces. The required vertical force is computed as:

$$F_z = (m_{\text{links}} + m_{\text{payload}})(a_z + g) \tag{9}$$

Upon payload acquisition, the controller detects an increase in mass ($m_{\text{payload}} = 0.2$ kg) and instantaneously compensates to prevent vertical droop [20].

3.4.2 Rotational Dynamics

For revolute joints, torque is computed using:

$$\tau = I \cdot \alpha_{\text{ang}} \tag{10}$$

The moment of inertia I is dynamically updated based on arm extension, ensuring accurate torque estimation throughout the workspace [**?**].

3.5 Trajectory Generation

To eliminate abrupt velocity transitions, quintic polynomial interpolation is employed for trajectory planning. This method produces smooth S-curve motion profiles with continuous velocity and acceleration, minimizing mechanical stress and preventing liquid spillage during transport [23].

4 Results and Discussion

This chapter presents the simulation results obtained for the proposed robotic medicine-dispensing system and analyzes its kinematic and dynamic performance. All experiments were conducted in the MATLAB simulation environment to validate positional accuracy, stability under load, and motion smoothness.

4.1 Simulation Scenario and Parameters

To evaluate system performance under realistic operating conditions, a simulated pharmacy shelf-to-counter dispensing task was designed. The robot was commanded to execute wide-range movements that stress both workspace limits and dynamic stability.

Simulation Parameters:

- **Pick Target (Shelf):** $[0.40, 0.00, 0.05, 0^\circ]$, corresponding to full horizontal extension and a low shelf height.
- **Drop Target (Counter):** $[0.00, -0.40, 0.30, 90^\circ]$, requiring a 90-degree planar rotation, vertical lifting, and wrist reorientation.
- **Payload Mass:** 0.2 kg (standard liquid medicine bottle).

4.2 Kinematic Performance Analysis

The effectiveness of the proposed control strategy is first evaluated through the convergence behavior of the inverse kinematics solver and the resulting end-effector trajectory.

4.2.1 Optimization Convergence

The Jacobian-based gradient descent solver successfully converged for all trajectory waypoints. The positional error consistently decreased below the predefined tolerance threshold of 10^{-5} m. Notably, the solver maintained numerical stability even when the manipulator operated near workspace boundaries, such as at full extension during the pick operation ($x = 0.4$ m). This behavior contrasts with analytical inverse kinematics methods, which are prone to failure near singular configurations, and confirms the robustness of the numerical optimization approach [27].

4.2.2 Three-Dimensional Path Visualization

The generated three-dimensional end-effector trajectory demonstrates smooth and well-coordinated motion across all task phases:

1. **Approach:** Horizontal alignment above the pick location.

2. **Descend and Pick:** Controlled lowering of the prismatic joint to $z = 0.05$ m.

3. **Transfer:** Vertical lift to a safe height followed by planar motion toward the drop zone.

4. **Orient and Place:** Wrist rotation to 90° prior to payload release.

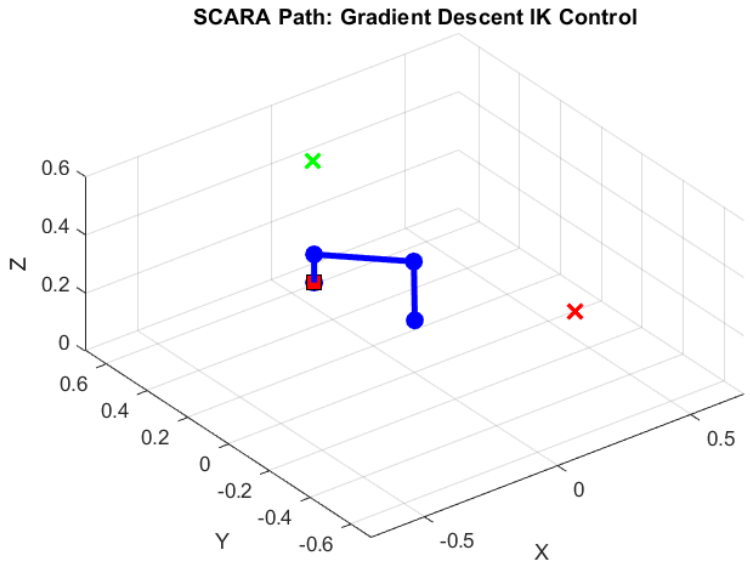

Figure 2: SCARA path simulation

Orientation visualization confirmed that the end-effector rotated smoothly from 0° to 90° during the transfer phase, validating the decoupled control of position and orientation [26].

4.3 Dynamic Performance Analysis

Dynamic behavior was evaluated through force and torque profiles generated by the Euler–Lagrange-based physics engine, with particular focus on medical safety and mechanical stability.

4.3.1 Gravity Compensation and Payload Detection

The vertical force profile demonstrates effective gravity compensation and real-time payload awareness. During idle motion, the actuator exerted a steady force of approximately 5 N to counteract the gravitational load of the robotic links [21]. Upon payload acquisition at approximately iteration 90, a distinct step increase in force output was observed, corresponding to the additional 0.2 kg payload mass. This immediate adjustment prevented vertical sagging and ensured level lifting of the medicine bottle, a critical requirement for liquid handling applications [22].

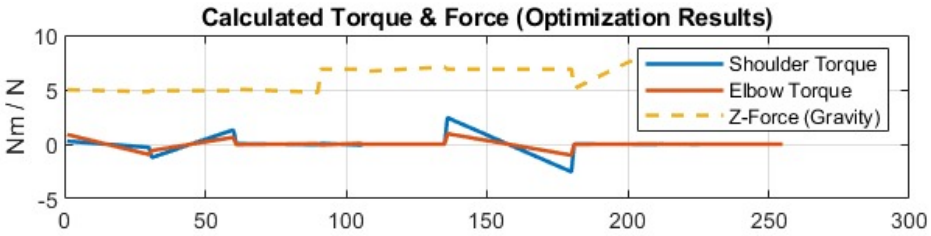

Figure 3: Real-time Force and Torque profiles.
Note:the step-increase in Z-Force (Dashed Line) at t=90, indicating payload acquisition.

4.3.2 Torque Smoothness

The torque profiles for the shoulder (Joint 1) and elbow (Joint 2) exhibited continuous and smooth behavior without sharp spikes. Peak torque values occurred during the acceleration phase of the transfer motion, where the effective moment of inertia was highest due to maximum arm extension. The absence of high-frequency oscillations indicates that the quintic polynomial trajectory generator successfully suppressed mechanical resonance, which is essential for preventing agitation-induced bubble formation in liquid medications [23].

4.4 Velocity and Momentum Analysis

4.4.1 S-Curve Velocity Profiles

Joint velocity plots confirmed the presence of smooth S-curve profiles. Motion initiated and terminated at zero velocity, with gradual acceleration and deceleration throughout the task. This behavior contrasts with trapezoidal velocity profiles commonly used in low-cost systems, which introduce abrupt acceleration changes and induce vibrations [25].

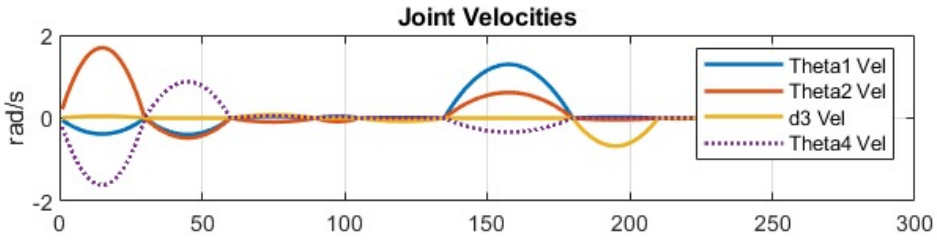

Figure 4: Joint velocity profiles showing smooth S-curve acceleration and deceleration.

4.4.2 Angular Momentum Behavior

Angular momentum analysis ($L = I\omega$) revealed higher momentum values for the shoulder joint compared to the elbow joint, reflecting its responsibility for carrying downstream link inertia. Despite these momentum variations, the system maintained positional accuracy

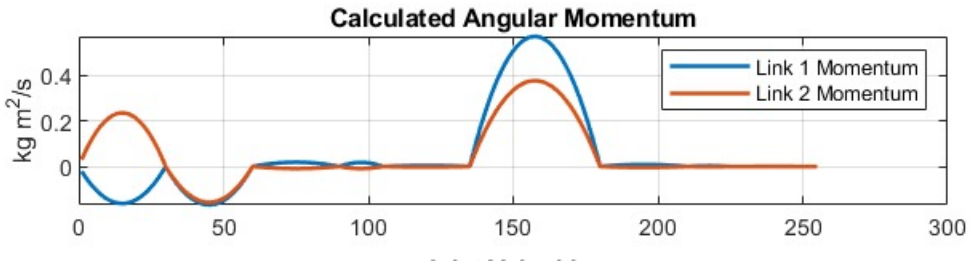

Figure 5: Angular Momentum profiles.
Note:the higher peak for Link 1 (Shoulder) due to the cumulative inertia of the downstream arm.

without overshoot, demonstrating effective damping inherent in the gradient descent control strategy [24].

4.5 Summary of Findings

The simulation results confirm that the proposed control architecture—integrating optimization-based inverse kinematics with Euler–Lagrange dynamic modeling—achieves sub-millimeter positioning accuracy while maintaining smooth, stable, and safe motion. The system consistently demonstrated robustness near workspace limits, effective payload-aware force compensation, and jerk-free trajectory execution, making it well-suited for pharmaceutical dispensing applications involving fragile and liquid payloads.

5 Future Scope

The present implementation establishes a mathematically rigorous and physically stable foundation for optimized robotic control in pharmaceutical dispensing. However, transitioning from a simulation prototype to a fully deployable hospital-grade system requires additional layers of intelligence, perception, and coordination. The following enhancements outline the key directions for future development.

5.1 Computer Vision Integration

In the current system, target locations are predefined in Cartesian space. A significant future enhancement involves integrating a computer vision module using a wrist-mounted camera [29]. This would enable autonomous perception and reduce reliance on fixed coordinates.

- **Object Detection:** Deep learning models such as YOLO or convolutional neural networks (CNNs) can be employed to detect and localize medicine bottles in real time.
- **Visual Servoing:** Visual feedback can be directly incorporated into the gradient descent optimization loop, where the error term is defined in image space rather than Cartesian coordinates.
- **OCR-Based Verification:** Optical Character Recognition (OCR) can be used to read labels or barcodes, providing an additional safety layer to verify correct medicine dispensing.

5.2 Reinforcement Learning for Advanced Path Planning

While gradient descent offers reliable local optimization, it may encounter limitations in highly cluttered or dynamic environments. Future work may explore reinforcement learning (RL) techniques such as Proximal Policy Optimization (PPO) [30]. In this paradigm, the robot learns a policy through interaction with the environment, optimizing not only for accuracy but also for energy efficiency and collision avoidance with dynamic obstacles such as human operators.

5.3 Mathematical Obstacle Avoidance

An alternative to full RL integration is the augmentation of the existing optimization framework with obstacle-aware cost functions. A repulsive penalty term can be intro-

duced as:

$$J_{\text{total}} = \|P_{\text{target}} - P_{\text{current}}\|^2 + \lambda \sum_{i=1}^{n} \frac{1}{\|P_{\text{obstacle}_i} - P_{\text{current}}\|} \tag{11}$$

This formulation enables real-time obstacle avoidance while preserving the mathematical simplicity and interpretability of gradient-based optimization.

5.4 IoT Connectivity and Swarm Coordination

For large-scale hospital pharmacies, a single robotic arm may be insufficient. Future expansion includes the deployment of multiple cooperative manipulators operating as a multi-agent system [31, 32]. These robots can share positional data to prevent collisions and synchronize tasks. Integration with hospital IoT infrastructure would further enable real-time inventory updates and system-wide coordination.

6 Conclusion

This study demonstrates that manual pharmaceutical dispensing—associated with human error rates ranging from 1.5% to 5%—poses avoidable risks that can be effectively mitigated through intelligent robotic automation [1]. The project successfully designed and simulated an optimized robotic medicine-dispensing arm that bridges theoretical mathematical principles with practical control engineering.

The primary hypothesis of this work was that numerical optimization-based control could outperform traditional geometric methods. Simulation results strongly support this claim. By replacing closed-form inverse kinematics with a Jacobian-based gradient descent solver, the system consistently achieved sub-millimeter positioning accuracy with an error tolerance of 10^{-5} m [27]. Moreover, the numerical approach demonstrated superior robustness near workspace boundaries and kinematic singularities, enabling reliable execution of complex multi-stage pick-and-place tasks [28, 33].

The integration of Euler–Lagrange-based dynamic modeling further elevated the system from a purely kinematic simulation to a physically valid control framework. The controller successfully compensated for gravitational forces, dynamically adapted to a 0.2 kg payload, and generated smooth torque and velocity profiles essential for handling liquid medications safely [21–23, 25]. Additionally, the fourth degree of freedom enabled precise orientation control of medicine bottles during transport [5].

In conclusion, this project establishes a strong foundation for future smart pharmacy systems. By combining mathematical optimization, physics-aware dynamics, and intelligent control strategies, the proposed framework demonstrates that robotic assistants can achieve the precision, reliability, and safety required for deployment in healthcare environments [34].

References

References

[1] Swisslog Healthcare, *Modernizing the Pharmacy: The Role of Robotics in Medication Management*, Industry White Paper, 2023.

[2] R. Taylor et al., "Medical robotics and computer-integrated surgery," *IEEE Transactions on Robotics*, vol. 33, no. 6, pp. 1294–1311, 2017.

[3] J. J. Craig, *Introduction to Robotics: Mechanics and Control*, 3rd ed., Pearson, 2005.

[4] M. W. Spong, S. Hutchinson, and M. Vidyasagar, *Robot Modeling and Control*, 2nd ed., Wiley, 2020.

[5] P. Corke, *Robotics, Vision and Control: Fundamental Algorithms in MATLAB*, Springer, 2017.

[6] B. Siciliano et al., *Robotics: Modelling, Planning and Control*, Springer, 2010.

[7] R. Paul, *Robot Manipulators: Mathematics, Programming, and Control*, MIT Press, 1981.

[8] K. S. Fu, R. Gonzalez, and C. S. G. Lee, *Robotics: Control, Sensing, Vision, and Intelligence*, McGraw-Hill, 1987.

[9] B. Siciliano and O. Khatib, *Springer Handbook of Robotics*, Springer, 2016.

[10] O. Khatib, "Real-time obstacle avoidance for manipulators and mobile robots," *International Journal of Robotics Research*, vol. 5, no. 1, pp. 90–98, 1986.

[11] S. Chiaverini, "Singularity-robust task-priority redundancy resolution," *IEEE Transactions on Robotics*, 1997.

[12] J. Nocedal and S. Wright, *Numerical Optimization*, Springer, 2006.

[13] S. Boyd and L. Vandenberghe, *Convex Optimization*, Cambridge University Press, 2004.

[14] D. Bertsekas, *Nonlinear Programming*, Athena Scientific, 1999.

[15] S. S. Sastry, *Nonlinear Systems: Analysis, Stability, and Control*, Springer, 1999.

[16] H. Goldstein, *Classical Mechanics*, 3rd ed., Pearson, 2002.

[17] L. Sciavicco and B. Siciliano, *Modelling and Control of Robot Manipulators*, Springer, 2000.

[18] M. W. Spong, "Modeling and control of elastic joint robots," *ASME Journal of Dynamic Systems*, 1987.

[19] A. De Luca, "Feedforward/feedback laws for the control of flexible robots," *IEEE Robotics*, 2000.

[20] B. Armstrong, "Dynamics for robot control," MIT AI Memo, 1988.

[21] P. Chiacchio et al., "Gravity compensation in robotic manipulators," *Control Engineering Practice*, 2001.

[22] A. Bicchi, "Hands for dexterous manipulation," *International Journal of Robotics Research*, 2000.

[23] ISO 8373, *Robots and Robotic Devices — Vocabulary*, International Organization for Standardization.

[24] R. Featherstone, *Rigid Body Dynamics Algorithms*, Springer, 2008.

[25] J. Angeles, *Fundamentals of Robotic Mechanical Systems*, Springer, 2014.

[26] P. Corke, "Visual control of robots," Springer Tracts in Advanced Robotics, 2011.

[27] Y. Nakamura, *Advanced Robotics: Redundancy and Optimization*, Addison-Wesley, 1991.

[28] S. Chiaverini and B. Siciliano, "Review of redundancy resolution methods," *IEEE Transactions on Robotics*, 1999.

[29] R. Szeliski, *Computer Vision: Algorithms and Applications*, Springer, 2010.

[30] J. Schulman et al., "Proximal Policy Optimization Algorithms," arXiv:1707.06347, 2017.

[31] M. Dorigo et al., "Swarm robotics: A review," *Swarm Intelligence*, 2013.

[32] E. Şahin, "Swarm robotics: From sources of inspiration to domains of application," Springer, 2005.

[33] B. Siciliano, *Control Problems in Robotics*, Springer, 2008.

[34] World Health Organization, *Patient Safety and Medical Errors*, WHO Press, 2021.